High-order parameterization of (un)stable manifolds for hybrid maps: implementation and applications

Vincent Naudot [*1], J.D. Mireles James [†1], and Qiuying Lu [‡3]

[1]Florida Atlantic University, Department of Mathematical Sciences, 777 Glades Road, 33431 Boca Raton, FL, USA
[3]Department of Mathematics, Zhejiang Sci-Tech University, Hangzhou, Zhejiang, 310018, CN

March 29, 2016

Abstract

In this work we study, from a numerical point of view, the (un)stable manifolds of a certain class of dynamical systems called hybrid maps. The dynamics of these systems are generated by a two stage procedure: the first stage is continuous time advection under a given vector field, the second stage is discrete time advection under a given diffeomorphism. Such hybrid systems model physical processes where a differential equation is occasionally kicked by a strong disturbance. We propose a numerical method for computing local (un)stable manifolds, which leads to high order polynomial parameterization of the embedding. The parameterization of the invariant manifold is not the graph of a function and can follow folds in the embedding. Moreover we obtain a representation of the dynamics on the manifold in terms of a simple conjugacy relation. We illustrate the utility of the method by studying a planar example system.

1 Introduction

Stable and unstable manifolds associated with hyperbolic invariant sets are fundamental objects of study in dynamical systems theory [1]. In addition to describing the motion of orbits near invariant sets, intersections between stable and unstable manifolds provide global information about movement between

[*]Email: vnaudot@fau.edu

[†]J.M.J partially supported by NSF grant DMS - 1318172 Email: jmirelesjames@fau.edu

[‡]L. partially supported by NNSF grant 11101370 and '521' talent program of ZSTU, No. 11430132521304. Email: qiuyinglu@163.com

different regions of phase space. In some cases these intersections force the existence of complicated chaotic motions [2, 3, 4]. Owing to their importance in both theoretical and practical applications, there is a substantial literature on numerical methods for computing (un)stable manifolds. A thorough review of the literature is beyond the scope of the present work, and we refer the interested reader to the review article [5], the historical appendix of [6], and also the recent book of [7] for more scholarly discussion of the existing methods and literature.

One approach to computing invariant manifolds is to develop some high order expansions for a chart map or parameterization. High order methods are useful as they provide a smooth and accurate representation of the manifold away from the hyperbolic invariant set. Many such methods have been developed and applied directly to dynamical systems given by diffeomorphisms or vector fields. See for example [8] for (un)stable manifolds of hyperbolic fixed points for diffeomorphisms, [9, 10] for (un)stable manifolds of equilibrium solutions of differential equations, [11] for (un)stable manifolds of invariant circles for diffeomorphisms, [12, 13, 14] for (un)stable manifolds of periodic orbits for vector fields. Moreover, the list above is by no means complete and we direct the interested reader again to [7] and also to [15].

In the present work we develop a higher order scheme for studying (un)stable manifolds for hybrid dynamical systems which are given neither by an explicit map nor an explicit vector field. The systems we consider have dynamics generated by composition of a continuous flow with a discrete time map. Such systems can be thought of as the composition of two maps: the time T map for a flow which is then composed with a given fixed map. The complication is that the time T map is only implicitly defined by the vector field, hence the composition dynamics are not generated by a closed analytic expression. Similarly, the hybrid dynamical system cannot be seen as a time T map of a single vector field. This state of affairs rules out the use of many of the standard analytic methods mentioned above.

In order to describe the problem more precisely we establish some notation. We say that a map

$$\mathbf{f} : \mathbb{R}^n \to \mathbb{R}^n, \ \mathbf{x} \mapsto \mathbf{f}(\mathbf{x}),$$

is a *hybrid map* if there exists a vector field $\mathcal{X}$ define on $\mathbb{R}^n$ and an affine map,

$$\mathbf{L} : \mathbb{R}^n \to \mathbb{R}^n, \ \mathbf{x} \mapsto \mathbf{L}(\mathbf{x}),$$

such that

$$\mathbf{f}(\mathbf{x}) = \mathbf{L} \circ \mathcal{X}_1(\mathbf{x}),$$

where $\mathcal{X}_t$ stands for the flow of $\mathcal{X}$ at the time t. Furthermore, in the case when n is even, we say that such a map is a *Hamiltonian based hybrid map* if $\mathcal{X}$ is Hamiltonian.

From the qualitative point of view, such maps play an important role in dynamical systems. For example the Hénon map appears in this way, as we

recall in Example 1 below. Actually, hybrid maps generalize a large class of system, and admit complex phenomena such as chaos and strange attractors [16]. Hybrid maps are also important in biology, for instance when modeling the dynamics of Caribbean coral reefs [17] when the kick represents a strong change in the environment for example due to the presence of periodic huricannes.

In this article we restrict our study to the two-dimensional case and compute asymptotic expansions of local (un)stable manifolds of fixed points of hybrid systems. Again, the challenging aspect of this task comes from the fact that it is in general impossible to express such map explicitly or asymptotically near a specific point. Before describing the strategy and stating the main results of this article, we revisit the case of the Hénon map [18] and recall some basics concerning (un)stable manifolds.

1.1 The Hénon map as Hybrid map

The Hénon map can be defined as follow

$$H_{a,b} : \mathbb{R}^2 \to \mathbb{R}^2,\ (x, y) \mapsto (1 - ax^2 + y, bx), \quad a, b \in \mathbb{R}.$$

We now show that, up to a conjugacy, the Hénon map is a Hamiltonian based hybrid map. Define the following vector field

$$\mathcal{X} :\ \dot{x} = x, \qquad \dot{y} = -y + k - \beta x^2.$$

It is easy to verify that the above vector field is Hamiltonian with first integral Hamiltonian

$$F(x, y) = xy - kx + \frac{\beta}{3}x^3,$$

and with respect to the standard symplectic structure $w = dx \wedge dy$. The flow of the above vector field can be computed directly, i.e., we have

$$x(t) = x(0)e^t, \quad y(t) = y(0)e^{-t} + k(1 - e^{-t}) + \frac{\beta}{3}x(0)^2(e^{-t} - e^{2t}).$$

In other words

$$\mathcal{X}_t(x, y) = \left(xe^t, ye^{-t} + k(1 - e^{-t}) + \frac{\beta}{3}x^2(e^{-t} - e^{2t})\right).$$

Consider now the following linear map

$$L(x, y) = (y, bx).$$

We then have

$$L \circ \mathcal{X}_t(x, y) = \left(ye^{-t} + k(1 - e^{-t}) + \frac{\beta}{3}x^2(e^{-t} - e^{2t}), bxe^t\right).$$

By choosing

$$k = \frac{1}{1 - e^{-1}}, \quad \beta = \frac{a}{3(e^2 - e^{-1})}, \text{ and } \ t = 1,$$

we get

$$L \circ \mathcal{X}_1(x,y) = \Big(ye^{-1} + 1 - ax^2, bex \Big),$$

which is conjugate to the Hénon map above via the following transformation

$$\psi(x,y) = (x, ey),$$

i.e.,

$$H_{a,b}(x,y) = \psi^{-1} \circ L \circ \mathcal{X}_1 \circ \psi(x,y).$$

1.2 Unstable manifold revisited

Let

$$\mathbf{g} : \mathcal{D} \subset \mathbf{R}^2 \to \mathbf{R}^2, \ \mathbf{x} \mapsto \mathbf{g}(\mathbf{x}),$$

be a smooth diffeomorphism defined in a neighborhood $\mathcal{D}$ of a fixed point of saddle type $\mathbf{p}$, i.e.,

$$\mathbf{g}(\mathbf{p}) = \mathbf{p}, \quad \text{Spect}(d\mathbf{g}(\mathbf{p})) = \{-\lambda, \mu\}, \quad \text{where} \quad -\lambda < 0 < \mu.$$

Without lost of generality, we can assume that $\mathbf{p}$ is the origin. The local unstable manifold of $\mathbf{g}$ at $\mathbf{p}$ admits a parametrization

$$W_u = \{W_u(t), \quad t \in \mathbb{R}\},$$

that satisfies, $W_u(0) = 0, \quad \dfrac{dW_u}{dt}(0) = \mathbf{V}_\mu$, and

$$W_u(\mu t) = \mathbf{g}(W_u(t)), \tag{1}$$

where $\mathbf{V}_\mu$ is an eigenvector of $d\mathbf{g}(0)$ associated to μ. Assume that $\mathbf{g}$ admits the following asymptotic

$$\mathbf{g}(x,y) = \sum_{(i,j)\in\mathbb{Z}^2} g_{i,j} x^i y^j, \ \text{where} \ \ g_{i,j} = (g_{i,j,1}, g_{i,j,2}).$$

Writing

$$W_u(t) = \sum_{n=1}^{\infty} \mathbf{W}_n t^n, \ \text{where} \ \mathbf{W}_n = (W_{n,1}, W_{n,2}),$$

by identifying terms on the left hand side of (1) with the terms on the right hand side, one deduces the $\mathbf{W}_n$'s by induction on n. See for instance [8] for the details in the case of the Hénon map, [4] for the cases of the standard quadratic map and the Bogdanov map, and [19] for the case of the infinite dimensional Kot-Schaffer map.

A similar approach is possible when $g = \mathcal{X}_1$, where $\mathcal{X}_s$ is the time s of a smooth vector field defined near a singularity of saddle type. This can be

achieved without computing the associated flow. Let $l_u > 0$ be the positive eigenvalue of the linearization of $\mathcal{X}$ at the singularity. Write

$$W_u(e^{l_u s}t) = \mathcal{X}_s(W_u(t)),\ s \in \mathbb{R},$$

and after differentiation with respect to s we get

$$l_u e^{l_u s} t W_u'(e^{l_u s}t) = \frac{d}{ds}\Big(\mathcal{X}_s(W_u(t))\Big),$$

and by setting $s = 0$ in the above equation we get

$$l_u t W_u'(t) = \mathcal{X}(W_u(t)). \tag{2}$$

Assuming that $\mathcal{X}$ has the form

$$\mathcal{X}(x,y) = \sum_{(i,j)\in\mathbb{Z}^2} X_{i,j,1} x^i y^j \frac{\partial}{\partial x} + X_{i,j,2} x^i y^j \frac{\partial}{\partial y}, \tag{3}$$

we identify terms on the left hand side of (2) with the terms on the right hand side of (3), and deduce the $\mathbf{W}_n$'s by induction on n, similarly as in the case of a diffeomorphism. See for example [20] for the details in the case of the Gray-Scott equation, and [21] for the case of the two dimensional (un)stable manifolds of the Lorenz system. See also [10, 22] for a discussion of the design and implementation of software which automates these formal computations.

However, in the case where g is the composition of flow and a diffeo, it is almost impossible (in general) to work out the asymptotics of g by hand via formal computations as described above. In order to obtain these asymptotics we proceed differently, and this is the main motivation of this article. In the next section, we develop a technique to compute the desired coefficients.

2 An algorithm

Before describing the procedure to compute such coefficients, we introduce some notations. Let $\mathbf{p} = (p_1, p_2)$ be a hyperbolic fixed point of an hybrid map $\mathbf{g}$. We denote by λ and μ the corresponding eigenvalues, i.e., $|\lambda| < 1 < |\mu|$, and $\mathbf{V}_\mu = (1, v_\mu)$ the corresponding (normalized) unstable eigenvector. Let $0 < r << 1$ be a small real number and denote

$$W^u = \{W^u(s), \quad -r < s < r\},\ (\text{and}\ \ W^s = \{W^s(s), \quad -r < s < r\}),$$

a parametrization of the (local) unstable (respectively stable) manifold of $\mathbf{g}$ at $\mathbf{p}$. Define the space

$$\mathcal{W} = \{W : (-r, r) \to \mathbf{R}^2,\ W(0) = \mathbf{p} \quad W'(0) = \mathbf{V}_\mu\}.$$

The set $\mathcal{W}$ is equipped with the C^0 topology, i.e,

$$d(W_1, W_2) = \sup_{-r\le s<\le r} \|W_1(s) - W_2(s)\|.$$

Let k be a positive integer. We also define the following operator

$$\Psi(W)(s) = \mathbf{g}^k\Big(W(\mu^{-k}s)\Big).$$

We now state the following proposition.

Proposition 1 *Let* $\mathbf{g}$, $\mathbf{p}$, μ *and* $\mathcal{W}$ *as above. Then, for* $r > 0$ *sufficiently small*

$$\lim_{n\to\infty} \Psi^n(W) = W^u,$$

for all $W \in \mathcal{W}$.

PROOF: Without lost of generality, we may assume that $p_1 = 0 = p_2$ and that the system of coordinates in which we express the map $\mathbf{g}$ and $W \in \mathcal{W}$ is such that

$$\{W^u(s),\ -r \le s \le r\} \subset \{x = 0\} \text{ and } \{W^s(s),\ -r \le s \le r\} \subset \{y = 0\}.$$

The map $\mathbf{g}$ takes the form

$$\mathbf{g}(x, y) = (\lambda x + x h_{1,1}(x, y), \mu y + y h_{2,1}(x, y)),$$

where $h_{1,1}(x, y)$ and $h_{2,1}(x, y)$ are smooth functions and

$$h_{1,1}(0, 0) = 0 = h_{2,1}(0, 0).$$

It follows that

$$\mathbf{g}^k(x, y) = (\lambda^k x + x h_{1,k}(x, y), \mu^k y + y h_{2,k}(x, y)),$$

where $h_{1,k}(x, y)$ and $h_{2,k}(x, y)$ are smooth functions and

$$h_{1,k}(0, 0) = 0 = h_{2,k}(0, 0).$$

Take $W \in \mathcal{W}$. We have

$$W(s) = (s + w_1(s), v_\mu s + w_2(s)),$$

where both w_1 and w_2 are smooth and satisfy

$$w_1(s) = \mathcal{O}(s^2) = w_2(s).$$

Therefore

$$W(\mu^{-k}s) = (\mu^{-k}s + \mu^{-2k}\bar{w}_1(s), \mu^{-k}v_\mu s + \mu^{-2k}\bar{w}_2(s)),$$

where

$$\mu^{-2k}\bar{w}_1(s) = w_1(\mu^{-k}s), \quad \mu^{-2k}\bar{w}_2(s) = w_2(\mu^{-k}s).$$

Thus

$$\mathbf{g}^k(W(\mu^{-k}s)) = \left((\frac{\lambda}{\mu})^k s + \lambda^k \mu^{-2k} \hat{w}_1(s) + \mu^{-k} \tilde{w}_1(s), v_\mu s + \mu^{-k} \hat{w}_2(s)) \right), \quad (4)$$

where $\hat{w}_1,\ \hat{w}_2,\ \tilde{w}_1$ are smooth functions. From (4), we get that

$$\mathbf{g}^k(W(\mu^{-k}s)) \to (0, v_\mu s),$$

in the C^0 topology, ending the proof of the proposition. □

As a consequence, it is sufficient to apply the above proposition to the line tangent to the unstable manifold at the fixed point i.e.,

$$W_0 = \{W_0(s) = \mathbf{p} + s\mathbf{V}_\mu\}.$$

Since we do not know $\mathbf{g}$ explicitly, getting the asymptotic of $\Psi(W_0)$ is hopeless. To overcome this difficulty, we choose and integer $M >> 1$ and (using the asymptotic developed in the next section) compute

$$\mathcal{W}_M = \{\hat{W}(s_j) = (w_{j,x}, w_{j,y}),\ \ s_j = -r + rj/M,\ j = 0, \ldots, 2M\}.$$

To get the asymptotic of $\hat{W}(s)$, we interpolate the sets

$$\{w_{j,x},\ j = 0, \ldots, 2M\},\ \{w_{j,y},\ j = 0, \ldots, 2M\},$$

with respectively $P_x(s)$ and $P_y(s)$, that are polynomial functions of degree $2M$. More precisely we construct (in a unique way) $P_x(s)$ and $P_y(s)$ such that

$$P_x(s_j) = w_{j,x},\ \ P_y(s_j) = w_{j,y},\ j = 0, \ldots, 2M.$$

We then define the new parametric curve $\hat{\Psi}(W)$

$$\hat{\Psi}(W)(s) = \left(P_x(s), P_y(s) \right),$$

and for all integer $n \geq 1$

$$W^n(s) = \hat{\Psi}(W^{n-1})(s) = \left(P_{x,n}(s), P_{y,n}(s) \right).$$

3 A study case

The remaining part of this section is devoted to illustrating the algorithm described above for a specific example. In what follow we assume $\mathbb{R}^2$ to be endowed with the standard symplectic structure $\Omega = dx \wedge dy$. We consider the following Hamiltonian

$$H(x, y) = bx^4/4 - x^2/2 + y^2/2,$$

leading to the following vector field

$$\mathcal{X} = y\frac{\partial}{\partial x} + (x - bx^3)\frac{\partial}{\partial y}, \quad (5)$$

or the following ODE

$$\dot{x} = y, \quad \dot{y} = x - bx^3, \tag{6}$$

where b is a parameter. We also define the following linear map

$$L(x, y) = (x + a_1, cy + a_2),$$

where a_1, a_2 and c are parameters. Our concern is with the map

$$\mathbf{g}(x, y) = L \circ \mathcal{X}_T(x, y), \tag{7}$$

where $\mathcal{X}_T$ is the time T-map associated with $\mathcal{X}$, where $T > 0$ is seen as yet another parameter. We choose specific values of the parameters a_1, a_2, b, c and T, see Figure 1 for more details. Using a Newton method we find a fixed point of $\mathbf{g}$ of saddle type $\mathbf{p}$. We apply the algorithm described in the former section to compute the asymptotics of the (un)stable manifolds of $\mathbf{g}$ at $\mathbf{p}$.

3.1 Flow and variational equation

A first task consists of computing the asymptotic of flow associated with $\mathcal{X}$. Our implementation uses a Taylor method [15, 22], although Runge-Kutta and any other symplectic integrator would provide similar results. We will need to compute the eigenvalues of $d\mathbf{g}(x, y) = dL \circ d\mathcal{X}_T(x, y)$ and associated eigenvectors. We solve the associated variational equation to compute $d\mathcal{X}_T(x, y)$. More precisely, assume $(x(t), y(t))$ is the solution of (6) with initial condition (x, y) We write

$$\frac{\partial x}{\partial x_0} = \xi_1, \ \frac{\partial x}{\partial y_0} = \xi_2, \ \frac{\partial y}{\partial x_0} = \zeta_1, \ \frac{\partial y}{\partial y_0} = \zeta_2,$$

and from (6) we deduce the following variational equation

$$\hat{\mathcal{X}} : \left\{ \begin{array}{rcl} \dot{x} & = & y \\ \dot{y} & = & x - bx^3 \\ \dot{\xi}_1 & = & \zeta_1 \\ \dot{\xi}_2 & = & \zeta_2 \\ \dot{\zeta}_1 & = & \xi_1 - 3bx^2\xi_1 \\ \dot{\zeta}_2 & = & \xi_2 - 3bx^2\xi_2 \end{array} \right. . \tag{8}$$

We consider the solution of (8) with initial condition

$$x(0) = x, \ y(0) = y, \ \xi_1(0) = 1, \ \xi_2(0) = 0, \ \zeta_1(0) = 0, \ \zeta_2(0) = 1.$$

It follows that

$$d\mathbf{g}(x, y) = dL \circ d\mathcal{X}_T(x, y) = \begin{pmatrix} \xi_1(T) & \xi_2(T) \\ c\zeta_1(T) & c\zeta_2(T) \end{pmatrix}. \tag{9}$$

For simplicity, we write

$$P = (x, y, \xi_1, \xi_2, \zeta_1, \zeta_2),$$

to denote the initial condition of (8). The Taylor expansion of the solution has the form

$$\hat{\mathcal{X}}_t(P) = \hat{\mathcal{X}}_{t,N}(P) + \mathcal{R}_{t,N}(P),$$

where

$$\hat{\mathcal{X}}_{t,N}(P) = \sum_{j=0}^{N} \mathbf{A}_j(P) t^j,$$

and N is a large integer (to be chosen appropriately depending upon the desired precision), and $\mathcal{R}_{t,N}(P)$ represents the reminder. The $\mathbf{A}_j$'s are vectors and are computed in such a way that $\hat{\mathcal{X}}_0(P) = (P)$, i.e., $\mathbf{A}_0(P) = (P)$ and

$$\frac{\partial}{\partial t}\hat{\mathcal{X}}_t(P) = \hat{\mathcal{X}}\left(\sum_{j=0}^{N} \mathbf{A}_j(P) t^j + \sum_{j=N}^{\infty} \mathbf{A}_j(P) t^j\right). \tag{10}$$

Thanks to (8), collecting term of order k in t on the left hand side of (10) and identifying these with the terms of order k in t on the right hand side leads to

$$\mathbf{A}_1(P) = \hat{\mathcal{X}}(P) = (y, x - bx^3, \zeta_1, \zeta_2, \xi_1 - 3bx^2\xi_1, \xi_2 - 3bx^2\xi_2),$$

and for all $k \geq 1$,

$$\mathbf{A}_{k+1} = (A_{k+1,1}, A_{k+1,2}, A_{k+1,3}, A_{k+1,4}, A_{k+1,5}, A_{k+1,6}) \tag{11}$$

$$= \begin{pmatrix} \dfrac{A_{k,2}}{k+1} \\ \dfrac{A_{k,1}}{k+1} - \dfrac{b}{k+1}\displaystyle\sum_{j=0}^{k} A_{k-j,1} \sum_{i=0}^{j} A_{i,1}A_{j-i,1} \\ \dfrac{A_{k,5}}{k+1} \\ \dfrac{A_{k,6}}{k+1} \\ \dfrac{A_{k,4}}{k+1} - \dfrac{3b}{k+1}\displaystyle\sum_{j=0}^{k} A_{k-j,3} \sum_{i=0}^{j} A_{i,1}A_{j-i,1} \\ \dfrac{A_{k,5}}{k+1} - \dfrac{3b}{k+1}\displaystyle\sum_{j=0}^{k} A_{k-j,4} \sum_{i=0}^{j} A_{i,1}A_{j-i,1} \end{pmatrix}. \tag{12}$$

Concerning the precision of this computation we expect the reminder to be of the same order as the 'first missing term', that is

$$\|\mathcal{R}_{t,N}(x,y)\| = \mathcal{O}\left(\|A_{N+1}\| t^{N+1}\right).$$

For values of t sufficiently small, $\hat{\mathcal{X}}_{t,N}$ is a good approximation of $\mathcal{X}_t$. However, when t becomes large, this approximation is no longer accurate. To solve this

problem we choose an integer large K and replace $\hat{\mathcal{X}}_{t,N}$ by iterating K times $\hat{\mathcal{X}}_{t/K,N}$, i.e.,

$$\hat{\mathcal{X}}_t \sim \hat{\mathcal{X}}_{t/K,N} \circ \hat{\mathcal{X}}_{t/K,N} \circ \cdots \circ \hat{\mathcal{X}}_{t/K,N}.$$

The map $\mathbf{g}$ defined in (7) is then approximated as follows

$$\mathbf{g}(x,y) \sim \mathbf{g}_{K,N}(x,y) = L \circ \mathcal{X}_{T/K,N}(x,y),$$

where $\mathcal{X}_{T/K,N}(x,y)$ represents the fist two components of $\hat{\mathcal{X}}_{T/K,N}(P)$. By choosing both K and N sufficiently large we guarantee the computation of $\mathbf{g}$ to the desired precision.

3.2 About precision and accuracy

Let $\mathbf{p}$ be a hyperbolic fixed point of $\mathbf{g}$ (that is of $\mathbf{g}_{K,N}$) of saddle type. The computation of the locus of this fixed point, together with the eigenvalues μ of $d\mathbf{g}(\mathbf{p})$ and the corresponding normalized eigenvectors can be achieved with arbitrarily high precision from (9) using Newton's method.

For r sufficiently small, the sequence $\{W^n\}_{n\geq 1}$ accumulates to the local unstable manifold of $\mathbf{p}$ containing that point, i.e., $\{W^u(s),\ -r \leq s \leq r.\}$. We illustrate the result of the above in Figure 1. To control the accuracy of our computation we proceed as follows. We first fix an integer $n_0 >> 1$.

- Choose K and N such that the map g is computed with n_0 digits precision. This can be achieved by verifying that for any randomly chosen point $\mathbf{q}$ close to the fixed point $\mathbf{p}$

  $$\|g_{K,N}(\mathbf{q}) - g_{K+1,N+1}(\mathbf{q})\| \leq 10^{-n_0-1}.$$

- Iterate the above algorithm n_2 times so that the n_0 first coefficients of $P_{n_2-1,x}$ (respectively $P_{n_2-1,y}$) and those of $P_{n_2,x}$ (respectively $P_{n_2,y}$) coincide.

- Re-run the above algorithm with different values of M and r and verify that this leads to the same result as before.

- Verify that by setting

  $$W^u(s) = (P_{n_2,x}(s), P_{n_2,y}(s)),$$

  we have

  $$\|\mathbf{g} \circ W^u(\mu^{-1}s) - W^u(s)\| \sim 10^{-n_0}.$$

- We observe that the bigger $|\mu|$ is the faster the convergence is. To accelerate the procedure we may want to choose k bigger.

In Figure 1 below, the global unstable manifold (red) is obtained by first computing the local unstable manifold following the algorithm described above and by replacing $W^u(s)$ by $\mathbf{g}^k(W^u(\mu^{-k})(s))$. The values of the parameter satisfy

$$a_1 = 0,\ a_2 = 1.95,\ b = 12.2,\ c = 0.9,\ T = 1.07. \tag{13}$$

The local unstable (red) manifold is obtained after $n_2 = 5$ iterations of the operator Ψ, with $k = 7$ and $n_0 = 30$. The global stable manifold (blue) is obtained by redoing the same as above knowing that it coincides with the unstable manifold of $\mathbf{g}^{-1}(x) = \mathcal{X}_{-T} \circ L^{-1}$. Those 2 manifolds are superimposed revealing transverse intersection and therefore chaos. The orbit of the map $\mathbf{g}(x) = L \circ \mathcal{X}_T$ starting from an arbitrary chosen point reveals the existence of a (strange) attractor for the system. Also superimposition of the unstable manifold and the attractor suggests that this attractor is contained in the closure of the unstable manifold, compare with [18] Figures 2 and 3 concern the same system but with different values of the time T and the dissipative factor c.

References

[1] M. W. Hirsch, C. C. Pugh, and M. Shub. *Invariant manifolds*. Lecture Notes in Mathematics, Vol. 583. Springer-Verlag, Berlin-New York, 1977.

[2] Jacob Palis and Floris Takens. *Hyperbolicity and sensitive chaotic dynamics at homoclinic bifurcations*, volume 35 of *Cambridge Studies in Advanced Mathematics*. Cambridge University Press, Cambridge, 1993. Fractal dimensions and infinitely many attractors.

[3] S. Smale. Differentiable dynamical systems. *Bull. Amer. Math. Soc.*, 73:747–817, 1967.

[4] V. Gelfreich and V. Naudot. Width of the homoclinic zone in the parameter space for quadratic maps. *Experiment. Math.*, 18(4):409–427, 2009.

[5] B. Krauskopf, H. M. Osinga, E. J. Doedel, M. E. Henderson, J. Guckenheimer, A. Vladimirsky, M. Dellnitz, and O. Junge. A survey of methods for computing (un)stable manifolds of vector fields. *Internat. J. Bifur. Chaos Appl. Sci. Engrg.*, 15(3):763–791, 2005.

[6] X. Cabré, E. Fontich, and R. de la Llave. The parameterization method for invariant manifolds. III. Overview and applications. *J. Differential Equations*, 218(2):444–515, 2005.

[7] A. Haro, M. Canadell, J-LL. Figueras, A. Luque, and J-M. Mondelo. *The parameterization method for invariant manifolds: from theory to effective computations*. (To appear), 2014.

[8] Valter Franceschini and Lucio Russo. Stable and unstable manifolds of the Hénon mapping. *J. Statist. Phys.*, 25(4):757–769, 1981.

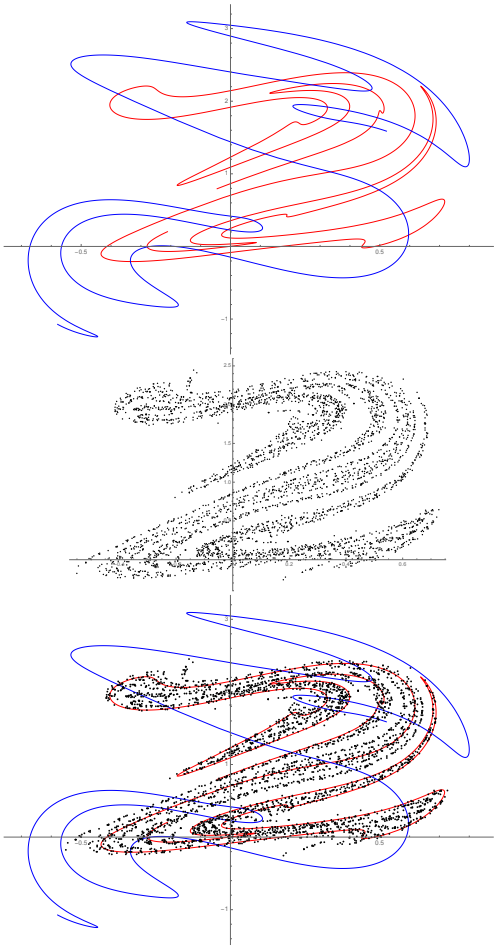

Figure 1: Top: The unstable manifold (red) for system (6) with stable manifold (blue). The fixed point is located at $(0.335, 1.026)$. Middle: an attractor of the system. Bottom: the unstable manifold superimposed with the attractor. Recall $T = 1.07$ and $c = 0.9$.

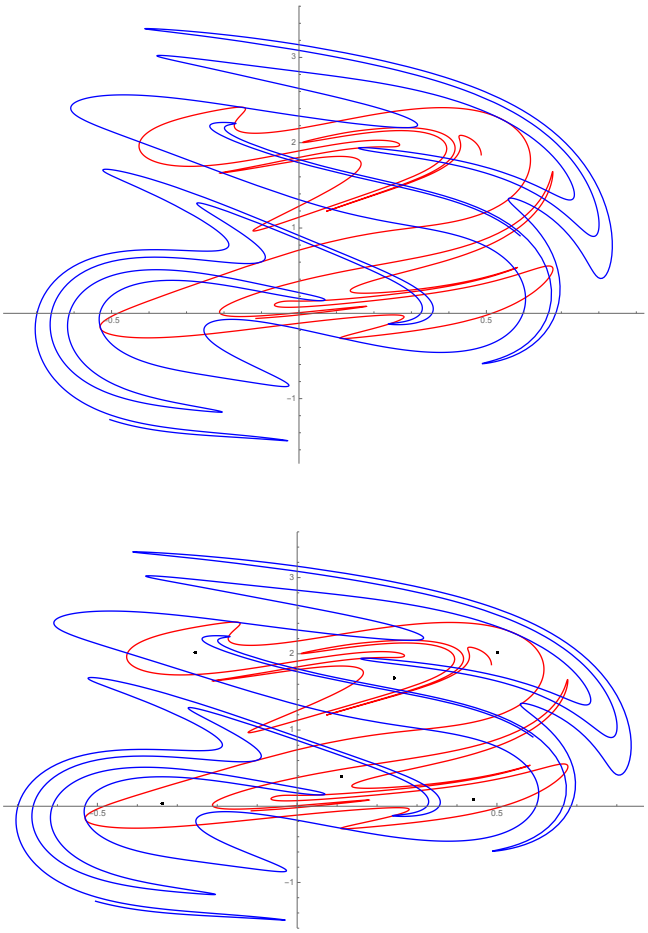

Figure 2: Top: the unstable manifold (red) with the stable manifold. Observer that both manifolds are almost tangent at several points. The fixed point is located at $(0.322, 1.01)$. Here $t = 1.1$ and $c = 0.93$. Bottom: superimposition of the invariant manifolds with the attractor which now consists of 6 periodic points.

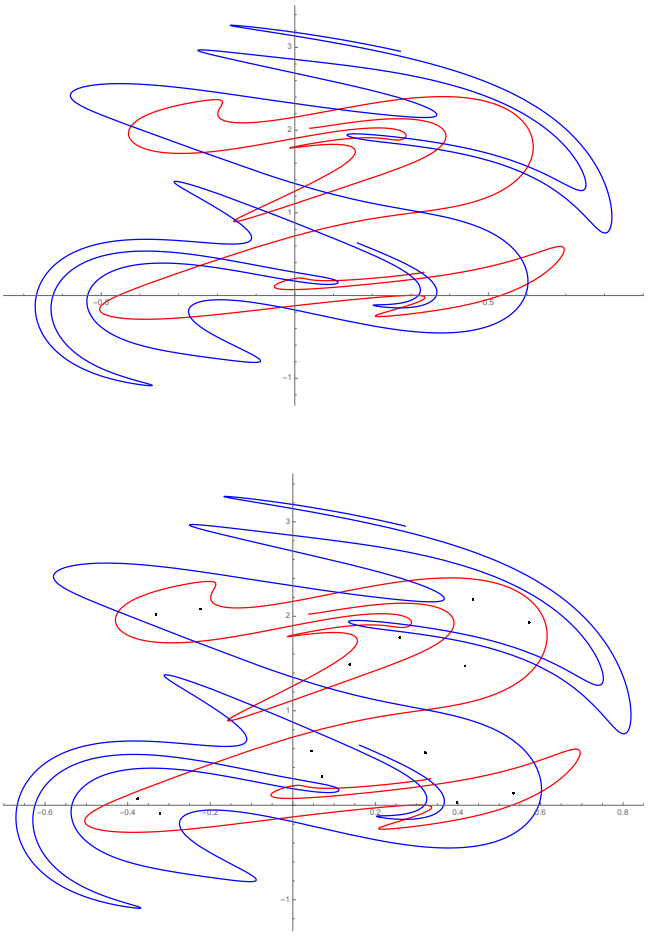

Figure 3: Top: the unstable manifold (red) with the stable manifold. The fixed point is located at $(0.317, 1.01)$. Here $T = 1.11$ and $c = 0.93$. Bottom: superimposition of the invariant manifolds with the attractor which now consists of 14 periodic points.

[9] Wolf-Jürgen Beyn and Winfried Kleß. Numerical Taylor expansions of invariant manifolds in large dynamical systems. *Numer. Math.*, 80(1):1–38, 1998.

[10] A. Haro. Automatic differentiation methods in computational dynamical systems: Invariant manifolds and normal forms of vector fields at fixed points. *Manuscript*.

[11] À. Haro and R. de la Llave. A parameterization method for the computation of invariant tori and their whiskers in quasi-periodic maps: numerical algorithms. *Discrete Contin. Dyn. Syst. Ser. B*, 6(6):1261–1300 (electronic), 2006.

[12] Roberto Castelli, Jean-Philippe Lessard, and J. D. Mireles James. Parameterization of invariant manifolds for periodic orbits I: Efficient numerics via the Floquet normal form. *SIAM J. Appl. Dyn. Syst.*, 14(1):132–167, 2015.

[13] Gemma Huguet and Rafael de la Llave. Computation of limit cycles and their isochrons: fast algorithms and their convergence. *SIAM J. Appl. Dyn. Syst.*, 12(4):1763–1802, 2013.

[14] Antoni Guillamon and Gemma Huguet. A computational and geometric approach to phase resetting curves and surfaces. *SIAM J. Appl. Dyn. Syst.*, 8(3):1005–1042, 2009.

[15] C. Simo. On the Analytical and Numerical Approximation of Invariant Manifolds. In D. Benest and C. Froeschle, editors, *Modern Methods in Celestial Mechanics, Comptes Rendus de la 13ieme Ecole Printemps d'Astrophysique de Goutelas (France), 24-29 Avril, 1989. Edited by Daniel Benest and Claude Froeschle. Gif-sur-Yvette: Editions Frontieres, 1990., p.285*, page 285, 1990.

[16] J. F. Heagy. A physical interpretation of the Hénon map. *Phys. D*, 57(3-4):436–446, 1992.

[17] S. Ippolito, V. Naudot, and E. Noonburg. Alternative stable states, coral reefs, and smooth dynamics with a kick. *Bulletin of Mathematical Biology*, (2016).

[18] M. Hénon. A two-dimensional mapping with a strange attractor. *Comm. Math. Phys.*, 50(1):69–77, 1976.

[19] J. D. Mireles James. Fourier-taylor approximation of unstable manifolds for compact maps: numerical implementation and computer assisted error bounds. *(submitted)*.

[20] Jan Bouwe van den Berg, Jason D. Mireles-James, Jean-Philippe Lessard, and Konstantin Mischaikow. Rigorous numerics for symmetric connecting orbits: even homoclinics of the Gray-Scott equation. *SIAM J. Math. Anal.*, 43(4):1557–1594, 2011.

[21] Jean-Philippe Lessard, Jason D. Mireles James, and Christian Reinhardt. Computer assisted proof of transverse saddle-to-saddle connecting orbits for first order vector fields. *J. Dynam. Differential Equations*, 26(2):267–313, 2014.

[22] Àngel Jorba and Maorong Zou. A software package for the numerical integration of ODEs by means of high-order Taylor methods. *Experiment. Math.*, 14(1):99–117, 2005.